Applied Surface Science 434 (2018) 1183–1192

Contents lists available at ScienceDirect

Applied Surface Science

journal homepage: www.elsevier.com/locate/apsusc

Full Length Article

UV-blocking properties of Zn/ZnO coatings on wood deposited by cold plasma spraying at atmospheric pressure

L. Wallenhorst[a,*], L. Gurău[b], A. Gellerich[c], H. Militz[c], G. Ohms[a], W. Viöl[a,d]

[a] University of Applied Sciences and Arts, Laboratory of Laser and Plasma Technologies, Von-Ossietzky-Straße 99, 37085 Göttingen, Germany
[b] Transilvania University of Braşov, Faculty of Wood Engineering, Str. Universităţii nr. 1, corp L, Braşov, Romania
[c] University of Göttingen, Wood Biology and Wood Products, Faculty of Forest Sciences, Büsgenweg 4, 37075 Göttingen, Germany
[d] Fraunhofer Institute for Surface Engineering and Thin Films, Application Center for Plasma and Photonics, Von-Ossietzky-Str. 100, 37085 Göttingen, Germany

ARTICLE INFO

Article history:
Received 4 September 2017
Received in revised form 11 October 2017
Accepted 30 October 2017
Available online 31 October 2017

Keywords:
Photostabilisation
Wood
Plasma coatings
Zinc oxide
ATR-FTIR
Surface roughness

ABSTRACT

In this study, artificial ageing of beech wood coated with Zn/ZnO particles by means of a cold plasma spraying process as well as coating systems including a Zn/ZnO layer and additional conventional sealings were examined. As ascertained by colour measurements, the particle coatings significantly decreased UV light-induced discolouration. Even though no significant colour changes were observed for particle-coated and alkyd-sealed samples, ATR-FTIR measurements revealed photocatalytic degradation of the alkyd matrix. In contrast, the polyurethane sealing appeared to be stabilised by the Zn/ZnO coating. Furthermore, morphologic properties of the pure particle coatings were studied by SEM and roughness measurements. SEM measurements confirmed a melting and solidifying process during deposition.

1. Introduction

As one of the oldest construction materials, wood is gaining even more importance with respect to contemporary demands for sustainability. Hence, the further development of wood products plays a major role in material science. In outdoor use however, wood and wood products are subjected to biotic and abiotic damage such as degradation by UV light. Many tropical wood exhibits a good resistance to biotic degradation mechanisms, yet its limited availability and the negative connotation regarding the destruction of tropical forests make its use undesirable. In contrast, most of the temperate wood species show a poor dimensional stability when faced with changes in temperature and humidity, a limited resistance to fungi and bacteria [1,2], and a particularly high sensitivity to UV light [1,3–5].

Consequently, the development of highly efficient protective wood coatings is the subject of intense current research. Particularly to protect wood from photodegradation, inorganic UV absorbers such as ZnO and TiO_2 have been widely studied and have proven to successfully protect the surface [6–9]. The use of (nano-) particles may, however, lead to an unintentional release of nanoparticles caused e. g. by abrasion due to airborne sand particles. These nanoparticles may be harmful for both human health and the (aquatic) environment [10,11]. Another challenge is represented by the photocatalytic activity of many UV absorbers that can lead to the degradation of organic matrix materials [12–16].

Among the emerging wood coating techniques are plasma-assisted processes. Various studies have addressed the generation of hydrophobic plasma polymers [17–20]. Furthermore, a plasma can be used to directly deposit solid powder material even on thermosensitive materials like wood [21–24]. In a previous study [24], thin particle coatings based on elemental Zn powder were deposited on glass substrates. Their characterisation revealed a mixed system of Zn and ZnO which led to a significantly reduced transmittance of light in the UV range. Based on these results, the present study investigates UV-blocking properties of similar coatings on beech wood (here referred to as “particle coating”). Additionally, coating systems composed of a particle coating and a conventional sealing (alkyd/polyurethane) were studied. The sequential application of UV absorbers and a sealing permits a precise dosage of UV absorbers and should at the same time inhibit nanoparticle release due, for example, to abrasion.

In this study, the UV-protective properties of Zn/ZnO coatings deposited in a cold plasma spraying process on beech wood were

* Corresponding author.
E-mail address: lena.wallenhorst@hawk-hhg.de (L. Wallenhorst).

https://doi.org/10.1016/j.apsusc.2017.10.214

Table 1
Summary of varied coating parameters to generate a thin coating (A) and a thick coating (B).

Coating no.	Powder feed rate in cm^3/h	Substrate displacement in mm/s
A	16.1	80
B	24.1	50

examined. In addition to the pure particle coatings, two coating systems involving a particle coating and a conventional top sealing (alkyd or polyurethane) were tested to eventually develop a coating system that permits a precise dosage of these UV absorbers and inhibits nanoparticle release from both leaching and abrasion. The effect of UV irradiation on the surfaces was assessed by colour and ATR-FTIR measurements.

Moreover, the morphology of such coatings was studied by means of SEM and surface roughness measurements.

2. Materials and methods

2.1. Materials

To carry out the UV tests, different coating systems were applied to beech wood samples (*Fagus sylvatica* L.) with dimensions 15 x 7 x 5 cm^3. In addition to the reference samples, Zn/ZnO coatings were deposited by cold plasma spraying as described below. Since the pure Zn/ZnO coatings do not exhibit a sufficient leach resistance, two commercially available sealing systems were tested along with unsealed samples. The used alkyd paint (ProfiDur Klarlack, Schöner Wohnen Farbe) represents a standard outdoor paint for wooden surfaces. Furthermore, the polyurethane (PUR) SKresin P34 NV from S u. K Hock GmbH was applied to investigate a second type of coating system. Three replicates were prepared for each coating system.

To study the roughness of particle-coated samples, one concentration (coating B, see below) of particles was also applied to beech wood samples of the size $6 \times 10 \times 4\ cm^3$ as well as to polypropylene samples ($6 \times 10 \times 3\ cm^3$).

Zinc particles with a diameter $d_{50} = 16\ \mu m$ were provided by ECKART GmbH. These particles feature an irregular shape and were found to improve the coating's homogeneity compared to the flake-like particles that were used previously [24].

2.2. Deposition process

The particle coatings were applied by means of a setup as described earlier [21–24]. In short, dry Zn particles were added to the afterglow of a jet discharge operated at atmospheric pressure while the sample was moved below the spraying nozzle by a xy linear stage to ensure an overall coating. The plasma source had an ignition voltage of approx. 15 kV and an effective voltage of 2–3 kV. Its maximum input power amounted to 2 kW and pulses were generated at a frequency of 50 kHz with a duration of 5–10 μs. Compressed air was used as the process gas. To generate a particle aerosol, the uniformly compressed powder was moved towards a rotating brush at a constant velocity which defined the feed rate. Finally, an air stream took up the powder above the brush to carry the particle aerosol towards the discharge. The carrier gas pressure was set to 0.16 MPa. During the deposition, the process gas flow was kept constant at 30 L/min. The distance between the spraying nozzle and the sample amounted to 16 mm. Table 1 lists parameters for the two coatings that were varied to obtain two different concentrations. This specific plasma source significantly limits substrate heating compared to conventional plasma spraying and therefore permits coating of thermosensitive materials. On the other hand, it restricts applicable powders to those featuring a melting temperature of less than approx. 1500 °C. Therefore, zinc particles were used as the base material instead of directly depositing ZnO powder.

2.3. Morphologic characterisation

Roughness measurements were performed for uncoated (kept as control) as well as particle-coated surfaces (coating B) of beech specimens ($6 \times 10 \times 4\ cm^3$, previously processed by planning), as well as for polypropylene samples ($6 \times 10 \times 3\ cm^3$). Wood is an example of a surface with inherent anatomical irregularities (for example wood pores), while polypropylene is a homogeneous material chosen for comparisons of the effect of the particle coating on surface morphology. For the roughness measurements, a Mar-Surf XT20 measuring system with XT 20 Topography manufactured by MAHR Göttingen GmbH was used. The instrument was endowed with a scanning head MFW 250 with tracing arm in the range of ±500 μm and a stylus with 2 μm tip radius and 90° tip angle. The specimens were measured at a speed of 0.5 mm/s, at a vertical resolution of 7 nm, a lateral resolution of 1 μm, and with a low scanning force of 0.7 mN. Both for coated and uncoated materials, five replicates were measured by randomly tracing three profiles per sample with a length of 70 mm, so that 15 profiles were available for evaluation of each combination of treatment and material. In the case of beech specimens, the measurements were carried out perpendicular to the grain direction, which corresponds to the direction of the highest roughness [25]

Roughness represents the finer irregularities of the surface texture that are usually inherent in a machining process and represented the target of this study in order to see by comparison with reference samples if any modification in surface morphology was caused by treating the surface with zinc particles. In order to obtain the surface roughness, the measured profiles must be filtered from other types of irregularities. In this sense, a Robust Gaussian Regression Filter contained in ISO/TS 16610-31:2010 [26] was used. This filter was tested and found suitable for wood surfaces [27,28].

After filtering, a range of roughness parameters were calculated for the profiles, such as: *Ra*, *Rq*, *Rt*, from ISO 4287 [29] and *Rk*, *Rpk*, *Rvk* from ISO 13565–2 [30]. *Ra* and *Rq* are mean parameters (the arithmetic mean of the absolute ordinate values, *Ra*, and the root mean square value of the ordinate values, *Rq*) most commonly used. *Rt* is the total height of the profile calculated as the sum of the maximum profile peak height and the largest absolute value profile valley depth and is expected to be sensitive to variations in local wood anatomy. *Rk* measures the core roughness of a profile, is the parameter least biased by inherent variation in wood anatomy and should best indicate the modifications in roughness caused by coating the surface. *Rpk* is the reduced peak height and represents the average height of the protruding peaks above the core roughness profile. *Rvk* is the reduced valley depth and represents the average depth of the profile valleys projecting through the core roughness profile. Both parameters are sensitive to outlying irregularities, as fuzziness in the case of *Rpk* and outlying deep anatomical valleys in the case of *Rvk* [31].

For treated and untreated surfaces and each roughness parameter, a mean value and the standard deviation were calculated. ANOVA with single factor was performed to test significant differences between reference samples and those treated with zinc particles.

Moreover, the particle coatings' morphology was examined by Scanning Electron Microscopy (SEM, JSM-5600LV from Jeol USA, Inc). All samples were sputter coated with a thin (approx. 32 nm) gold layer and measured at an accelerating voltage of 12 or 15 kV.

Table 2
Roughness parameters (mean values) and standard deviations for untreated and particle-coated beech surfaces (values in microns).

Sample	*Ra*	*Rq*	*Rt*	*Rk*	*Rpk*	*Rvk*
Reference beech	5.7	8.6	72.3	12.0	6.5	18.4
stdev	0.30	0.65	8.11	0.92	0.90	1.56
Particle-coated beech	6.2	9.1	80.4	13.67	9.12	17.89
stdev	0.24	0.48	7.50	1.66	1.63	2.22

Table 3
Roughness parameters (mean values) and standard deviation for untreated and particle-coated polypropylene surfaces (values in microns).

Sample	*Ra*	*Rq*	*Rt*	*Rk*	*Rpk*	*Rvk*
Reference polypropylene	0.019	0.028	1.101	0.056	0.027	0.038
stdev	0.001	0.009	0.837	0.003	0.005	0.015
Particle-coated polypropylene	5.325	7.370	61.622	14.068	12.405	2.098
stdev	0.287	0.343	9.417	1.385	0.703	1.115

2.4. Artificial ageing

Artificial ageing was simulated by a chamber for artificial weathering (QUV/Spray from Q-Lab Corporation) without using the spraying system and at a constant temperature of 50 °C. The solar irradiation intensity was set to 0.89 W/(m^{2}nm) at the lamp's emission peak around 340 nm (290 nm ≤ λ ≤ 400 nm) [32]. Three replicates were prepared for each coating system.

Colour measurements were performed by taking pictures under equal conditions and extracting colour parameters with the software Photoshop CS6. Constancy of illumination was confirmed by measurements with the spectroradiometer CS-200A (Konica Minolta). CIE Lab parameters were calculated on all three samples. In this colour system, L quantifies the lightness in grey-scale values from 0 to 100, whereas a and b represent the two colour axes. $\Delta a = a_0 - a_i > 0$ represents a green shift for the i-th measurement, $\Delta a < 0$ a red shift, $\Delta b = b_0 - b_i > 0$ a blue shift and $\Delta b < 0$ a yellow shift. The overall colour changes can be quantified by:

$$\Delta E = \sqrt{(L_0 - L_i)^2 + (a_0 - a_i)^2 + (b_0 - b_i)^2}.$$

Chemical changes caused by UV irradiation were examined by Attenuated Total Reflectance Fourier Transform Infrared Spectroscopy (ATR-FTIR, Perkin Elmer Frontier). Spectra were acquired for wavelengths ranging from 4000 to 400 cm^{-1} by performing 32 scans at a resolution of 4 cm^{-1}. All spectra were ATR and baseline corrected as well as normalised by use of the software Spectrum from Perkin Elmer. Moreover, slight smoothing was applied using a Savitzky-Golay filter (2nd degree polynomial). Measurements were carried out at identical spots before and after irradiation. For every coating system, a minimum of three measurements was obtained.

3. Results and discussion

3.1. Morphology of unsealed coatings

The surface roughness results are summarised in Table 2 and Table 3. From Table 2, it can be seen that the particle coating increased the surface roughness of beech. This increase is more reliably evaluated by the *Rk* parameter, because it is the parameter least biased by beech wood anatomy [33]. *Rk* increased with 13.6% in the case of particle-coated beech and this difference was significant for a 95% confidence interval ($p < 0.05$) according to the ANOVA test. In absolute values, this means a surface 1.64 μm rougher if coated. The fact that the surface was coated has generated, as expected, an increase in surface peaks as measured by the parameter *Rpk*, which exhibited the highest increase (41%) for coated beech compared to untreated surfaces. *Rvk*, which may be a measure of wood anatomical irregularities (mostly wood pores) for uncovered wood, decreased by 2.6% as compared to untreated beech, which is an indication that the particles may have penetrated into the wood anatomical cavities and obscuring them to a certain extent.

From Table 3, it can be observed that the particle coating caused a large increase in surface roughness of plastic surfaces for all measured parameters. For example, the *Rk* parameter increased 249 times, but the highest increase was recorded again for *Rpk* (461 times), while *Rvk* exhibited the minimum increase (55 times). This indicates that the particle coating increased the occurrence of isolated peaks on the surface for both polypropylene and beech surfaces. In comparison with polypropylene, the particles penetrate into the wood anatomical irregularities (gaps) and its overall effect on surface roughness is small.

To further study the coatings' morphology, SEM measurements were acquired. Fig. 1 shows representative images of the unmodified powder as well as the surfaces of both coating A and B (frame size: 48 x 64 μm^2).

For both coatings, the particles' shape differs significantly from the shape of the unmodified particles, confirming a melting and solidifying process as generally expected for plasma spraying techniques. In particular for thin coated samples (Fig. 1b), the wood structure was still clearly visible but even the thick coating did not completely obscure the original surface. Fig. 2 shows representative images of cross sections of the coatings confirming the formation of very flat particle shapes with thicknesses around or below 1 μm. The coating, being composed of several such particles with different thicknesses, appears to feature thicknesses around a few μm (approximately up to 5 μm).

3.2. Colour changes induced by UV irradiation

All samples were exposed to UV radiation for a total of 50 h with irradiation intervals ranging from 2 to 10 h. After each interval, pictures were taken to analyse colour changes.

The evolution of the total colour change ΔE of the different coating systems with increasing UV irradiation time is shown in Fig. 3. All values represent mean values of measurements on three samples.

For the unsealed as well as the PUR- and alkyd-sealed samples, a significant improvement of the colour stability is visible for the thin coated samples (A). Coating systems including a thick coating (B) only exhibit negligible colour changes. Likewise, all samples manifest a darkening by decreasing values for L (cf. Fig. 4), with strong changes for the reference samples, slight changes for thin coated samples and insignificant changes for thick coated samples. ΔE seemed to increase more strongly for PUR-sealed samples; therefore, it was tested for statistical significance. ANOVA, Bonferroni and Tukey-HSD all yielded a significant difference between the evolution of ΔE for unsealed as well as PUR-sealed samples on a level of $p = 0.05$. However, since only three samples were investigated for each coating system, the statistical evaluation may not be entirely reliable. The chromaticity parameters a and b (not shown) also reveal distinct changes (increasing redness and yellowness, respectively) for the coating systems without particles. Changes for samples covered with a thick coating remain negligible while thin coated samples exhibit very little colour changes compared to the uncoated samples. These colour changes of wood exposed to UV light are known to be generated by a decomposition and oxidation of lignin [3,5,34,35], which was observed also in our studies (see IR measurements below). Because of the similar evolution with increasing irradiation time, colour changes of uncoated but sealed

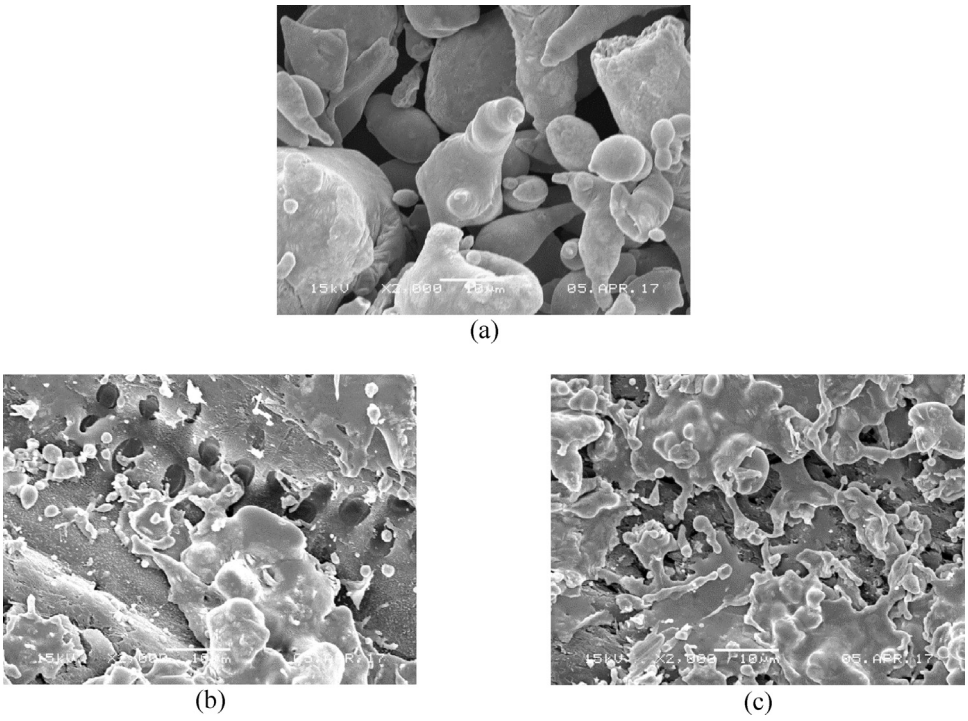

Fig. 1. SEM measurements on (a) untreated powder, (b) thin coated (A) and (c) thick coated (B) sample.

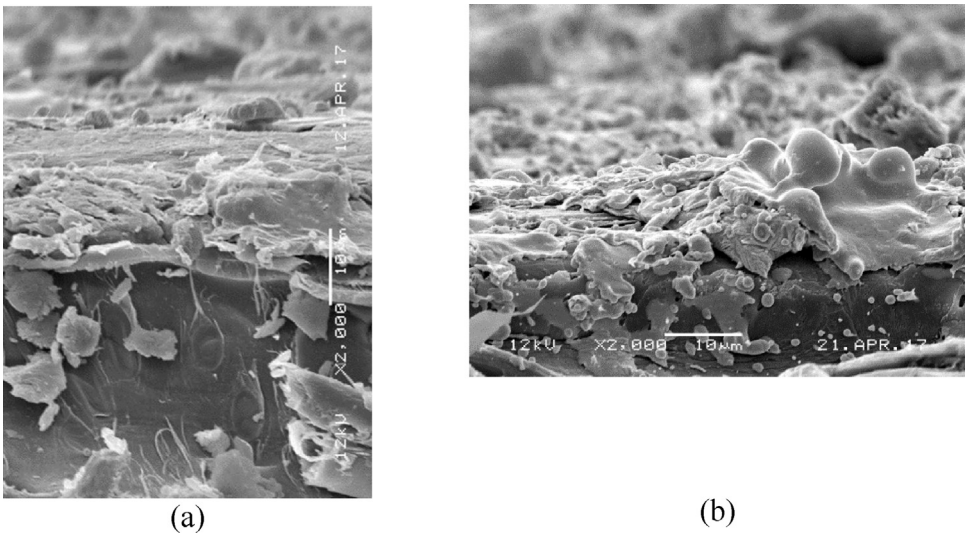

Fig. 2. SEM measurements of cross sections. (a): Thin coating A, (b): thick coating B.

samples are assumed to be mainly caused by chemical changes of the underlying wood sample.

3.3. Chemical changes induced by UV irradiation

Fig. 5 shows representative IR spectra of uncoated and unsealed wood before and after UV irradiation for 50 h along with the corresponding difference spectrum. Since the chemical changes are primarily visible in the fingerprint region, only the range from 1850 to 800 cm^{-1} is displayed. All spectra were normalised to the highest peak at 1028 cm^{-1} which features only a minor contribution from lignin [36,37] and mainly results from C—O stretching in cellulose and hemicellulose [37–40]. These components are known to be affected less by UV light than lignin [5]. Even though the wood structure was not entirely covered in the case of particle-coated samples, reliable ATR measurements were not possible since the coating prevented a sufficient contact between the wood surface and the ATR crystal. Therefore, only results for uncoated beech wood are discussed in absence of a sealing.

The results in this study coincide with changes reported in the literature [9,38,41–44]. Peaks mainly characteristic for lignin in wood are reduced, e. g. at 1596 cm^{-1} (C=C aromatic skeletal vibrations), and 1464 cm^{-1}/1422 cm^{-1} (C—H deformation). In particular the decreasing peak at 1503 cm^{-1} (C=C aromatic skeletal vibrations) confirms the degradation of lignin since it does not overlap considerably with peaks resulting from other wood components [45]. On the other hand, photooxidation is manifested in particular through a strong increase and broadening of the peak at 1730 cm^{-1} (C=O stretching vibration), indicating the formation of new and different carbonyl compounds [38,41,46] such as quinones

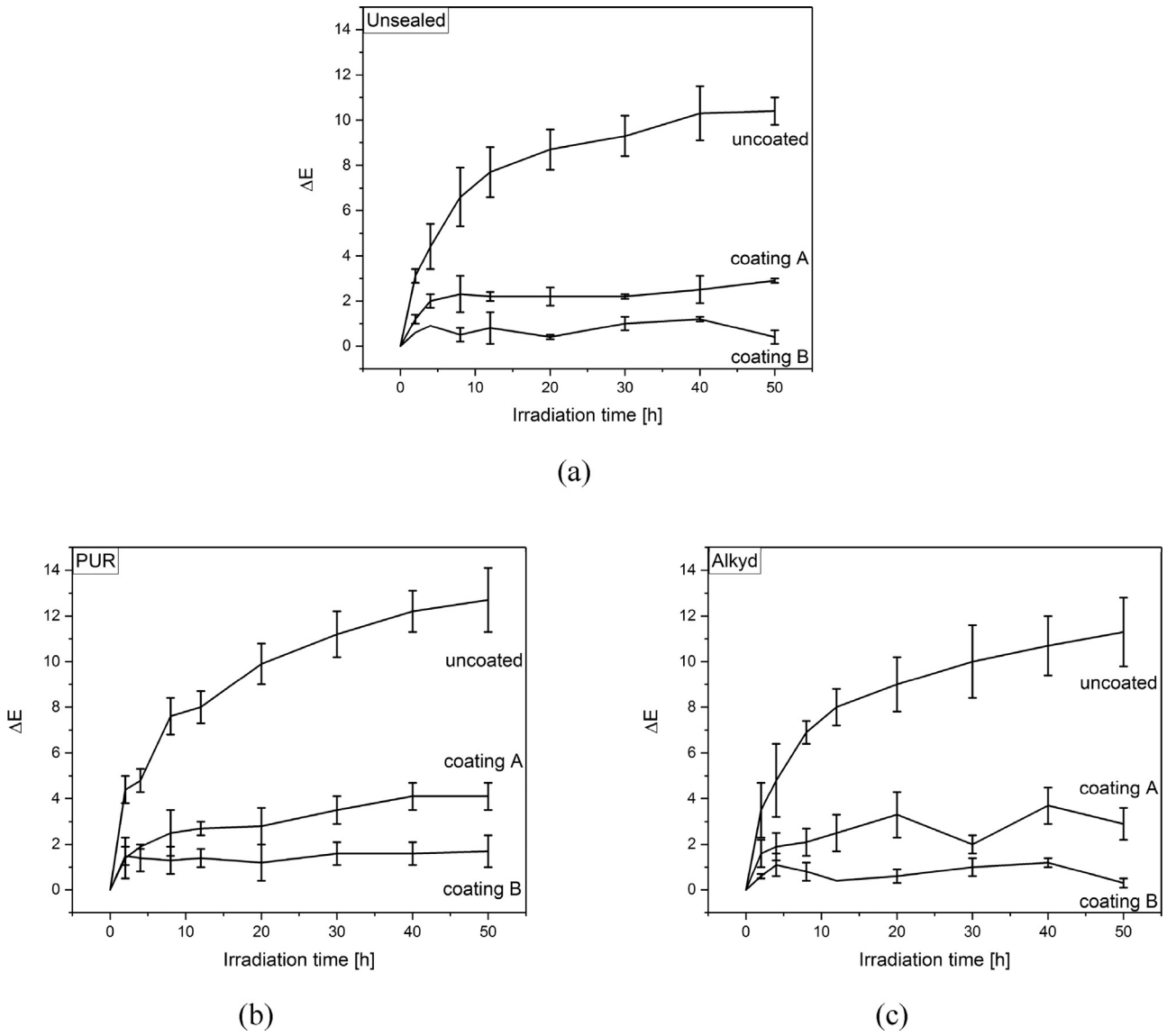

Fig. 3. Variation of total colour change with irradiation time. (a): Unsealed samples, (b): PUR-sealed samples, (c): alkyd-sealed samples.

which appear in the region below 1700 cm^{-1} [34]. The formation of these new chromophoric carbonyl groups is known to correlate well with UV light induced colour changes [34,35].

IR spectra of uncoated but PUR-sealed samples before and after irradiation are displayed in Fig. 6a.

Band assignment was done based on literature results [47–50]: Around 3700–3200 cm^{-1}, OH and NH stretching vibrations are evident. Methyl and methylene absorptions appear around 3000–2800 cm^{-1} and the carbonyl region is located approx. between 1800 and 1650 cm^{-1}. The peak at 1530 cm^{-1} may result from a coupling of NH bending vibrations with C—N stretching vibrations. C—O stretching and C—H bending vibrations are visible approx. from 1500 to 1100 cm^{-1}. All spectra were normalised to the highest peak at 1682 cm^{-1} (C=O).

Despite the slightly more pronounced colour changes, PUR-coated samples did not exhibit strong chemical changes after 50 h of UV irradiation. For PUR-sealed and uncoated samples, only minor changes in the methyl/methylene and carbonyl region occurred. The particle coatings seemed to have a stabilising effect on the coating system (cf. Fig. 6b and c). Therefore, a coating system composed of a Zn/ZnO particle coating and the PUR used in this study appears to be a promising approach to create UV-blocking layers on wooden surfaces.

In contrast, alkyd-sealed samples showed distinct chemical differences before and after UV irradiation. The relevant region in the IR range is depicted in Fig. 7 for representative measurements. All spectra were normalised to the highest peak at 1723 cm^{-1} generated by C=O stretching [51–53]; however, this peak was also affected by UV irradiation. Difference spectra are therefore not discussed. Despite this unavoidable inaccuracy, the main changes observed were in agreement with literature results as discussed below.

Without the presence of Zn/ZnO particles (cf. Fig. 7a), main changes were located at 2956 cm^{-1}, 2924 cm^{-1}, and 2853 cm^{-1} (C—H stretching, decreasing intensity). These changes may be attributed to an ongoing and terminating curing process involving the emission of volatile low molecular components under the influence of UV light as well as degradation processes through Norrish type I and II reactions [51,52]. The curing process in alkyd paints may even continue one month after its application to a surface [53,54]. The peak at 1261 cm^{-1} arises from O—C—O bonds in the polyester part of the alkyd [51,55] and decreased after the ongoing curing process and degradation during UV irradiation.

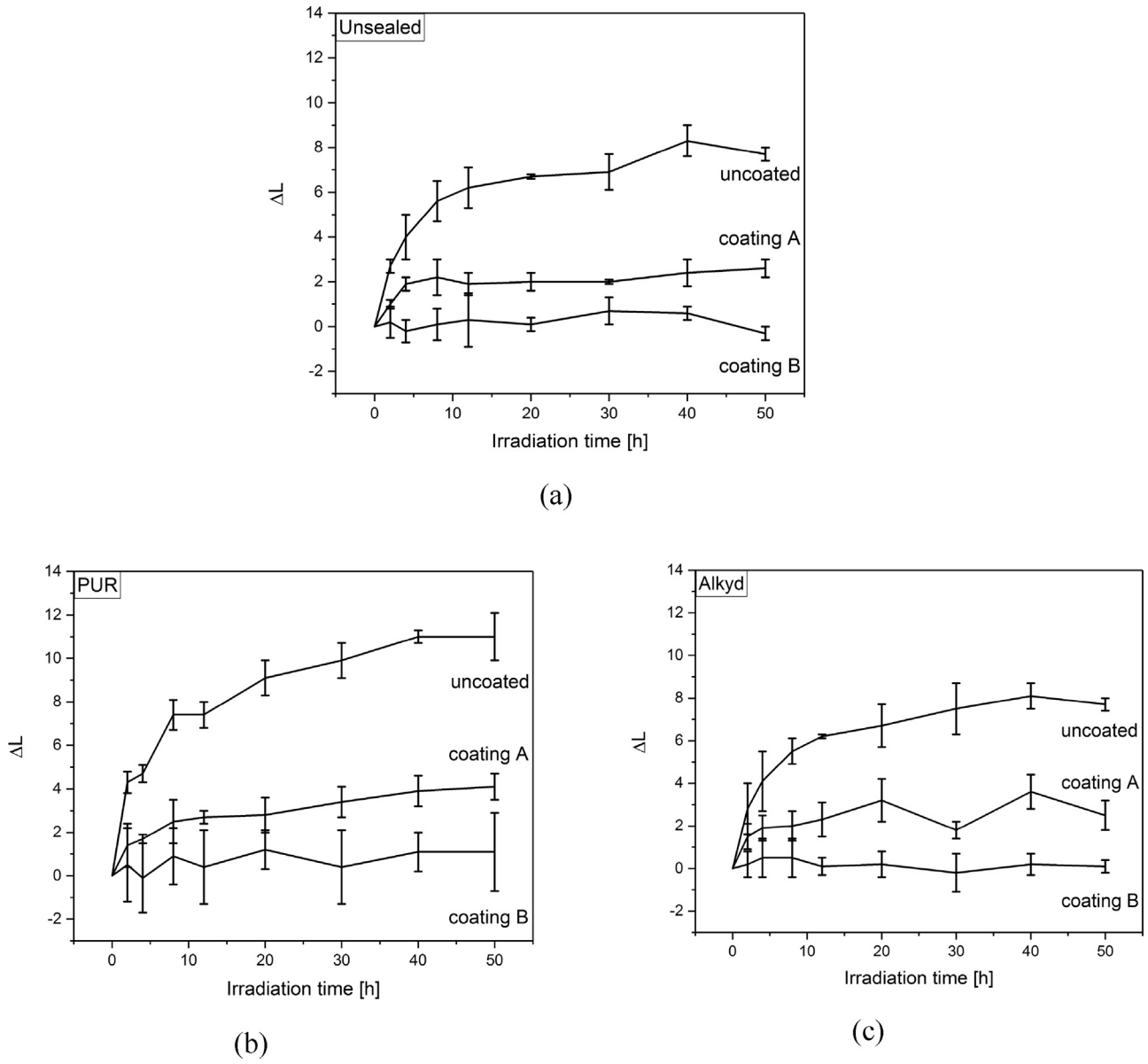

Fig. 4. Variation of the lightness L with irradiation time. (a): Unsealed samples, (b): PUR-sealed samples, (c): alkyd-sealed samples.

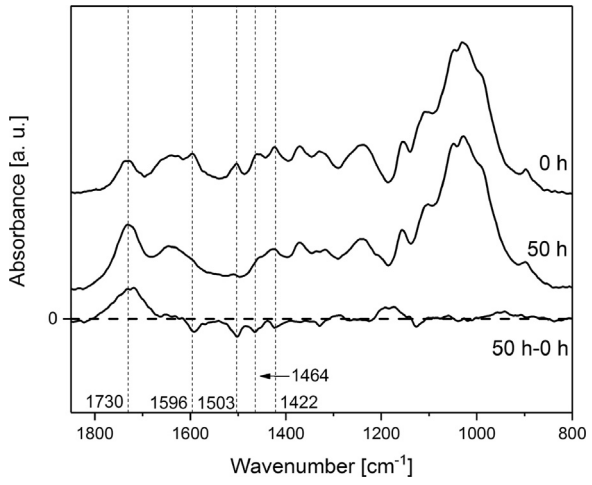

Fig. 5. IR fingerprint region of pristine (0 h) and irradiated (50 h) beech surfaces along with their difference spectrum (50 h–0 h).

Furthermore, a broadening of the peak at 1723 cm^{-1} took place, indicating the generation of new carbonyl compounds such as ketones, aldehydes or carboxylic acids [51,52]. The region between approx. 1300–900 cm^{-1} accounts for C—O/C—H bonds [53,56], and OH stretching vibrations are apparent through a broad peak around 3480 cm^{-1}.

The particle coatings appeared to intensify the degradation process, which is assumed to be due to the photocatalytic activity of ZnO [12–15]. For pigmented alkyd surfaces, the carbonyl peak that was used for normalisation is likely to be affected as well [55]; however, since all other peaks also change [51,55], it was kept as reference because it suffers less from overlaps with other peaks. Therefore, it has to be particularly taken into account that the spectra displayed only represent intensities relative to the C=O bond. Contrary to the unpigmented alkyd sealing, especially the OH peak showed a significant broadening with a new maximum around 3340 cm^{-1}. This peak may be attributed to the formation of carboxylic acids [55,57,58], which indicate an ageing process [52,58] that took place much faster than for the unpigmented paint.

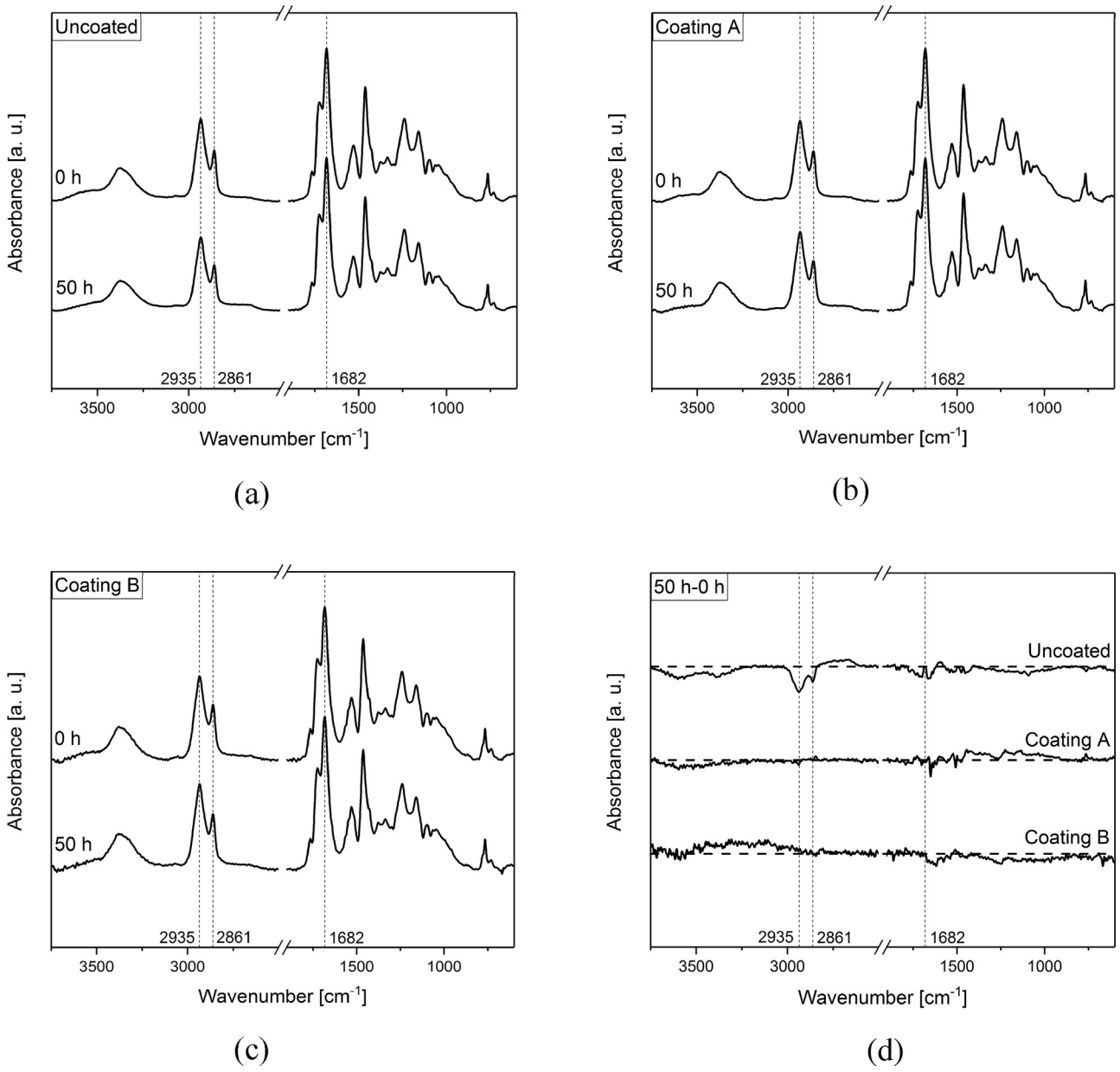

Fig. 6. IR spectra of PUR-sealed samples before and after irradiation. (a): Without particle coating, (b): thin particle coating, (c): thick particle coating, (d): resulting difference spectra for each coating system with dashed horizontal lines denoting zero values.

Due to a lack of information about the alkyd's specific composition, precise degradation processes cannot be named. Nevertheless, a couple of general pathways are discussed in the literature. The chemical changes may be partly explained by ongoing curing reactions (e. g. cross-linking, emission of volatile components) manifested for example by a decrease of methyl and methylene absorption [51,52]. The final alkyd film is susceptible to further reactions with radicals. Radicals can be formed through oxidative ageing involving β-scission, leading for example to the formation of aldehydes, alcohols and carboxylic acids [59,60] which were also visible in the spectra presented in this study. This result is in agreement with the shift of the carbonyl peak to smaller wavelengths. Norrish type I reactions may also lead to the formation of peroxy radicals and induce similar reactions as oxidative ageing involving β-scission [59,60]. Moreover, the carbonyl group may react through Norrish type II processes [51,59,60].

In summary, the chemical analysis confirmed degradation processes of uncoated and unsealed wood exposed to UV light. Alkyd sealings appeared to be distinctly affected by the irradiation process. Their application to particle-coated samples even led to accelerated ageing caused by photocatalytic degradation, making them unsuitable for a UV protective coating on wooden surfaces. In contrast, PUR-sealed samples without particle coatings exhibited only negligible changes in chemical structure. The prior application of a particle coating even stabilised the coating system and therefore represents a promising candidate for the further development of UV-blocking layers on wood and wood products.

4. Conclusion and outlook

In this study, Zn/ZnO coatings deposited by cold plasma spraying on wood and polypropylene were investigated with regard to morphologic aspects as well as their impact on photodegradation of wood and possible sealing materials. SEM measurements confirmed strong changes in the shape of the used particles following the deposition, thus confirming a melting and solidifying pro-

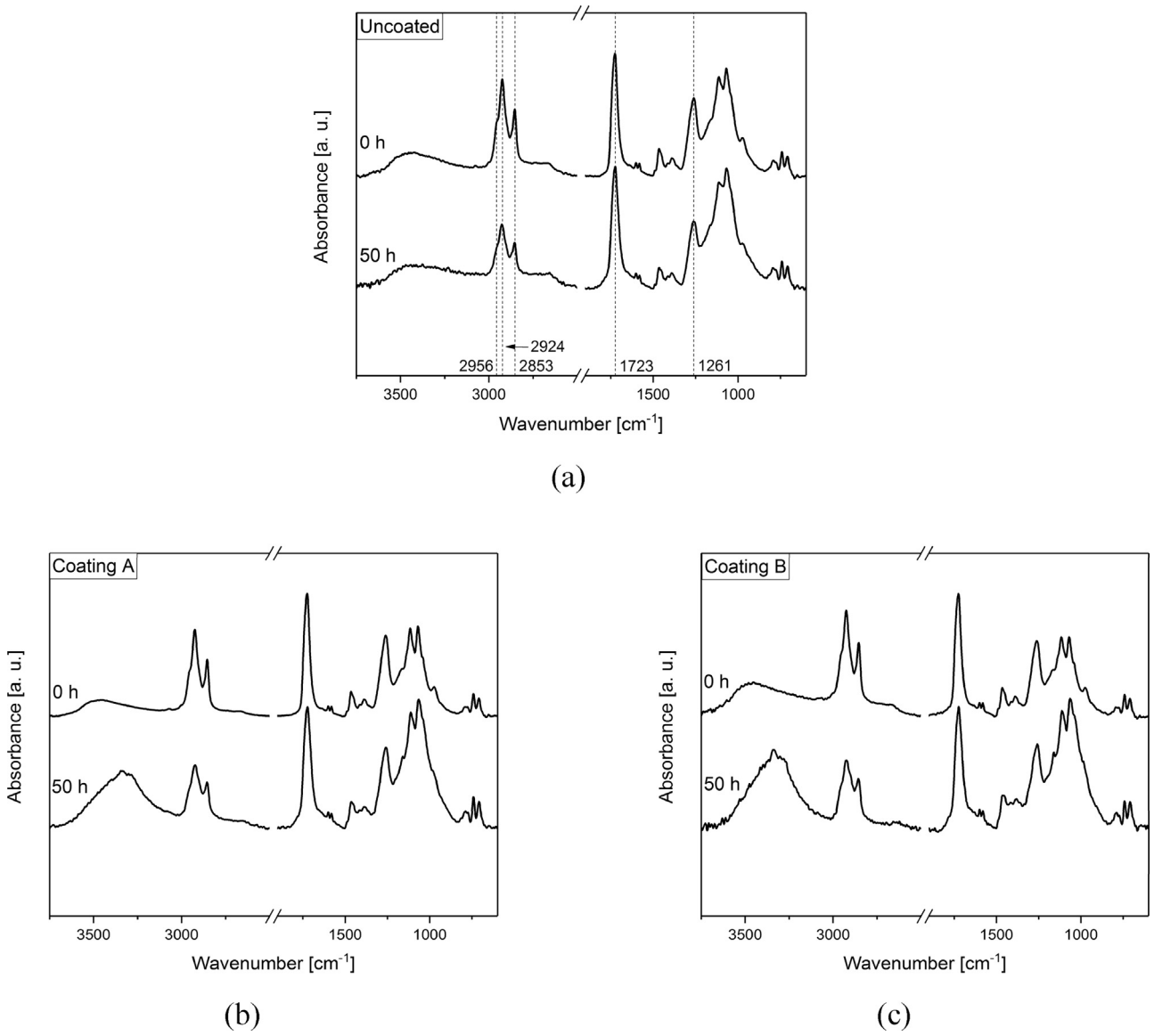

Fig. 7. IR spectra of alkyd sealed samples before and after irradiation. (a): Without particle coating, (b): thin particle coating, (c): thick particle coating.

cess. Moreover, a partial visibility of wood structure was affirmed. Roughness measurements showed a slight roughness increase for particle-coated beech, as measured by the *Rk* parameter, and a tendency of particles to increase the surface peaks as well as to reduce wood anatomical gaps, most probably by filling the wood pores to some extent.

The application of particle coatings significantly improved the colour stability of unsealed and alkyd- or PUR-sealed specimens. Whereas samples coated with concentration A still underwent minor discolouration upon UV irradiation, those coated with concentration B did not change. This behaviour was observed both for unsealed as well as for sealed beech wood samples, indicating that photocatalytic degradation of the matrix material by ZnO, though it did occur for alkyd-sealed samples, did not affect the colour within 50 h of UV irradiation.

Despite negligible discolouration, chemical analysis showed distinct changes for alkyd-sealed samples. Strong changes in the carbonyl region in addition to modifications in the C—O/C—H structure along with the appearance of OH bonds in carboxylic acids indicated photocatalytic degradation processes.

In contrast, the PUR matrix did not seem to be much affected by UV irradiation. Slight changes did occur to reference samples without particle coatings, but the application of Zn/ZnO coatings seemed to have stabilised the coating system.

Particularly the coating system including a Zn/ZnO particle coating along with the PUR sealing represents a promising approach to creating UV protective layers on wood in a relatively easy way. The used plasma setup operates at atmospheric pressure, requires relatively short treatment times and is suitable for coating thermosensitive materials like wood. Hence, the application of such a particle coating followed by a conventional sealing may be suitable for in-line processing. The sequential application of particles followed by a PUR sealing permits a precise dosage of UV-blocking filters and matrix material. Nanoparticle release due, for example, to leaching or abrasion is expected to be inhibited by such a coating system, but needs to be investigated in separate studies. Moreover, since ZnO features biocidal properties, the presented coating systems could therefore be tested as protective layers against bacteria and fungi.

Acknowledgements

Financial support from the Lower Saxony Ministry of Science and Culture is gratefully acknowledged. The authors further thank Max Baumung, Ghiath Jnido, Monika Gelker and Robert Koslowski for technical assistance, Roger Skarsten for proofreading the manuscript and ECKART GmbH for providing the used powder material. Moreover, the authors hereby acknowledge the structural funds project PRO-DD (POS-CCE, O.2.2.1., ID 123, SMIS 2637, ctr. No. 11/2009) for providing the infrastructure used in this work for surface roughness measurements.

Niedersächsisches Ministerium für Wissenschaft und Kultur

References

[1] M. Shimada, M. Takahashi, Biodegradation of cellulosic materials, in: Shiraishi Hon (Ed.), Wood and Cellulosic Chemistry, 1991.
[2] T.K. Kirk, E.B. Cowling, Biological Decomposition of Solid Wood, in: Rowell (Ed.), The Chemistry of Solid Wood, vol. 207, 1984, pp. 455–487.
[3] W.C. Feist, D.N.S. Hon, Chemistry of weathering and protection, in: Rowell (Ed.), The Chemistry of Solid Wood, vol. 207, 1984, pp. 401–451.
[4] B. George, E. Suttie, A. Merlin, X. Deglise, Photodegradation and photostabilisation of wood – the state of the art, Polym. Degrad. Stab. 88 (2) (2005) 268–274.
[5] D.N.S. Hon, Photochemistry of wood, in: Shiraishi Hon (Ed.), Wood and Cellulosic Chemistry, 1991.
[6] C.A. Clausen, F. Green, Nami kartal S: weatherability and leach resistance of wood impregnated with nano-zinc oxide, Nanoscale Res. Lett. 5 (9) (2010) 1464–1467.
[7] Y. Yu, Z. Jiang, G. Wang, Y. Song, Growth of ZnO nanofilms on wood with improved photostability, Holzforschung 64 (3) (2010).
[8] S.M. Fufa, B.P. Jelle, P.J. Hovde, Effects of TiO2 and clay nanoparticles loading on weathering performance of coated wood, Prog. Org. Coat. 76 (10) (2013) 1425–1429.
[9] J. Salla, K.K. Pandey, K. Srinivas, Improvement of UV resistance of wood surfaces by using ZnO nanoparticles, Polym. Degrad. Stab. 97 (4) (2012) 592–596.
[10] P.H.M. Hoet, I. Brüske-Hohlfeld, Salata O.V. Nanoparticles, - known and unknown health risks, J. Nanobiotechnol. 2 (1) (2004) 12.
[11] A. Baun, N.B. Hartmann, K. Grieger, K.O. Kusk, Ecotoxicity of engineered nanoparticles to aquatic invertebrates: a brief review and recommendations for future toxicity testing, Ecotoxicology 17 (5) (2008) 387–395.
[12] A. Rezaee, H. Rangkooy, A. Khavanin, A.J. Jafari, High photocatalytic decomposition of the air pollutant formaldehyde using nano-ZnO on bone char, Environ. Chem. Lett. 12 (2) (2014) 353–357.
[13] H.F. Moafi, A.F. Shojaie, M.A. Zanjanchi, Photocatalytic self-cleaning properties of cellulosic fibers modified by nano-sized zinc oxide, Thin Solid Films 519 (11) (2011) 3641–3646.
[14] C.A. Gouvêa, F. Wypych, S.G. Moraes, N. Durán, N. Nagata, P. Peralta-Zamora, Semiconductor-assisted photocatalytic degradation of reactive dyes in aqueous solution, Chemosphere 40 (4) (2000) 433–440.
[15] A. McLaren, T. Valdes-Solis, G. Li, S.C. Tsang, Shape and size effects of ZnO nanocrystals on photocatalytic activity, J. Am. Chem. Soc. 131 (35) (2009) 12540–12541.
[16] W.F. Sullivan, Weatherability of titanium-dioxide-containing paints, Prog. Org. Coat. 1 (2) (1972) 157–203.
[17] M. Bente, G. Avramidis, S. Förster, E.G. Rohwer, W. Viöl, Wood surface modification in dielectric barrier discharges at atmospheric pressure for creating water repellent characteristics, Holz als Roh- und Werkstoff 62 (3) (2004) 157–163.
[18] J. Profili, O. Levasseur, A. Koronai, L. Stafford, N. Gherardi, Deposition of nanocomposite coatings on wood using cold discharges at atmospheric pressure, Surf. Coat. Technol. (2016).
[19] G. Toriz, M.G. Gutiérrez, V. González-Alvarez, A. Wendel, P. Gatenholm, AdJ. Martínez-Gómez, Highly hydrophobic wood surfaces prepared by treatment with atmospheric pressure dielectric barrier discharges, J. Adhes. Sci. Technol. 22 (16) (2008) 2059–2078.
[20] S. Zanini, C. Riccardi, M. Orlandi, V. Fornara, M.P. Colombini, D.I. Donato, S. Legnaioli, V. Palleschi, Wood coated with plasma-polymer for water repellence, Wood Sci. Technol. 42 (2) (2008) 149–160.
[21] P. Gascón-Garrido, N. Mainusch, H. Militz, W. Viöl, C. Mai, Copper and aluminium deposition by cold-plasma spray on wood surfaces: effects on natural weathering behaviour, Eur. J. Wood Prod. (2016).
[22] P. Gascón-Garrido, N. Mainusch, H. Militz, W. Viöl, C. Mai, Effects of copper-plasma deposition on weathering properties of wood surfaces, Appl. Surf. Sci. 366 (2016) 112–119.
[23] L.M. Wallenhorst, S. Dahle, M. Vovk, L. Wurlitzer, L. Loewenthal, N. Mainusch, C. Gerhard, W. Viöl, Characterisation of PMMA/ATH layers realised by means of atmospheric pressure plasma powder deposition, Adv. Condens. Matter Phys. 2015 (3) (2015) 1–12.
[24] L.M. Wallenhorst, L. Loewenthal, G. Avramidis, C. Gerhard, H. Militz, G. Ohms, W. Viöl, Topographic, optical and chemical properties of zinc particle coatings deposited by means of atmospheric pressure plasma, Appl. Surf. Sci. 410 (2017) 485–493.
[25] L. Gurău, The roughness of sanded wood surfaces, in: Doctoral Thesis, 2004.
[26] International Organization for Standardization. Geometrical product specification (GPS) –Filtration – Part 31: Robust profile filters: Gaussian regression filters; (ISO/TS 16610-31:2010).
[27] L. Gurău, H. Mansfield-Williams, M. Irle, Filtering the roughness of a sanded wood surface, Holz als Roh- und Werkstoff 64 (5) (2006) 363–371.
[28] P.L. Tan, S. Sharif, I. Sudin, Roughness models for sanded wood surfaces, Wood Sci. Technol. 46 (1) (2012) 129–142.
[29] International Organization for Standardization, Geometrical product specifications (GPS). Surface texture: Profile method-Terms, definitions and surface texture parameters, (ISO 4287:1997 + Amd1: 2009).
[30] International Organization for Standardization, Geometrical product specifications (GPS) –Surface texture: Profile method. Surfaces having stratified functional properties. Part 2: Height characterisation using the linear material ratio curve; (ISO 13565-2:1996 + Cor 1:1998).
[31] E. Westkamper, A. Riegel, Qualitätskriterien für geschliffene massivholzoberflächen, Holz als Roh- und Werkstoff 51 (2) (1993) 121–125.
[32] Paints and varnishes - Coating materials and coating systems for exterior wood - Part 6: Exposure of wood coatings to artificial weathering using fluorescent UV lamps and water; (DIN EN 927-6:2016).
[33] L. Gurău, C. Csiha, H. Mansfield-Williams, Processing roughness of sanded beech surfaces, Eur. J. Wood Prod. 73 (3) (2015) 395–398.
[34] U. Müller, M. Rätzsch, M. Schwanninger, M. Steiner, H. Zöbl, Yellowing and IR-changes of spruce wood as result of UV-irradiation, J. Photochem. Photobiol. B 69 (2) (2003) 97–105.
[35] K.K. Pandey, Study of the effect of photo-irradiation on the surface chemistry of wood, Polym. Degrad. Stab. 90 (1) (2005) 9–20.
[36] O. Faix, Fourier transform infrared spectroscopy, in: Methods in Lignin Chemistry, 1992, pp. 83–109.
[37] P. Verma, U. Junga, H. Militz, C. Mai, Protection mechanisms of DMDHEU treated wood against white and brown rot fungi, Holzforschung 63 (3) (2009).
[38] C.-M. Popescu, M.-C. Popescu, C. Vasile, Structural analysis of photodegraded lime wood by means of FT-IR and 2D IR correlation spectroscopy, Int. J. Biol. Macromol. 48 (4) (2011) 667–675.
[39] H.G. Higgins, C.M. Stewart, K.J. Harrington, Infrared spectra of cellulose and related polysaccharides, J. Polym. Sci. 51 (155) (1961) 59–84.
[40] B. Mohebby, Application of ATR infrared spectroscopy in wood acetylation, J. Agric. Sci. Technol. 10 (3) (2008) 253–259.
[41] L. Calienno, A. Lo Monaco, C. Pelosi, R. Picchio, Colour and chemical changes on photodegraded beech wood with or without red heartwood, Wood Sci. Technol. 48 (6) (2014) 1167–1180.
[42] M.C. Timar, A.M. Varodi, L. Gurău, Comparative study of photodegradation of six wood species after short-time UV exposure, Wood Sci. Technol. 50 (1) (2016) 135–163.
[43] L. Tolvaj, O. Faix, Artificial ageing of wood monitored by DRIFT spectroscopy and CIE L*a*b* color measurements. 1. effect of UV light, Holzforschung 49 (5) (1995) 397–404.
[44] L. Tolvaj, C.-M. Popescu, Z. Molnar, E. Preklet, Effects of air relative humidity and temperature on photodegradation processes in beech and spruce wood, BioResources 11 (2016).
[45] K.K. Pandey, A study of chemical structure of soft and hardwood and wood polymers by FTIR spectroscopy, J. Appl. Polym. Sci. 71 (12) (1999) 1969–1975.
[46] D.N.-S. Hon, S.-T. Chang, Surface degradation of wood by ultraviolet light, J. Polym. Sci.: Polym. Chem. Edit. 22 (9) (1984) 2227–2241.
[47] H. Wang, Y. Wang, D. Liu, Z. Sun, Effects of additives on weather-Resistance properties of polyurethane films exposed to ultraviolet radiation and ozone atmosphere, J. Nanomater. (4) (2014) 1–7.
[48] H. Kim, M.W. Urban, Molecular level chain scission mechanisms of epoxy and urethane polymeric films exposed to UV/H 2 O. multidimensional spectroscopic studies, Langmuir 16 (12) (2000) 5382–5390.
[49] D. Rosu, L. Rosu, C.N. Cascaval, IR-change and yellowing of polyurethane as a result of UV irradiation, Polym. Degrad. Stab. 94 (4) (2009) 591–596.
[50] X. Yang, C. Vang, D. Tallman, G. Bierwagen, S. Croll, S. Rohlik, Weathering degradation of a polyurethane coating, Polym. Degrad. Stab. 74 (2) (2001) 341–351.
[51] F.X. Perrin, M. Irigoyen, E. Aragon, J.L. Vernet, Artificial aging of acrylurethane and alkyd paints: a micro-ATR spectroscopic study, Polym. Degrad. Stab. 70 (3) (2000) 469–475.
[52] V. Pintus, S. Wei, Schreiner M. Accelerated, UV ageing studies of acrylic, alkyd, and polyvinyl acetate paints: influence of inorganic pigments, Microchem. J. 124 (2016) 949–961.
[53] E.M. Salazar-Rojas, M.W. Urban, Curing of non-pigmented alkyd coatings detected by in-situ photoacoustic fourier transform infrared spectroscopy (PA FT-IR), Prog. Org. Coat. 16 (4) (1989) 371–386.
[54] M.W. Urban, E.M. Salazar-Rojas, Probing organic-inorganic interactions and curing processes in coatings by photoacoustic fourier transform infrared spectroscopy, J. Polym. Sci. A: Polym. Chem. 28 (6) (1990) 1593–1613.
[55] M. Anghelone, D. Jembrih-Simbürger, M. Schreiner, Influence of phthalocyanine pigments on the photo-degradation of alkyd artists' paints

under different conditions of artificial solar radiation, Polym. Degrad. Stab. 134 (2016) 157–168.
[56] J. van der Weerd, A. van Loon, Boon JJ: FTIR studies of the effects of pigments on the aging of oil, Stud. Conserv. 50 (1) (2005) 3–22.
[57] G. Socrates, Infrared and Raman Characteristic Group Frequencies: Tables and Charts, 3rd ed., John Wiley & Sons, Chichester, 2001.
[58] R. Ploeger, D. Scalarone, O. Chiantore, The characterization of commercial artists' alkyd paints, J. Cult. Heritage 9 (4) (2008) 412–419.
[59] S.M. Cakić, I.S. Ristić, J.M. Vladislav, J.V. Stamenković, D.T. Stojiljković, IR-change and colour changes of long-oil air drying alkyd paints as a result of UV irradiation, Prog. Org. Coat. 73 (4) (2012) 401–408.
[60] J. Mallégol, J.-L. Gardette, J. Lemaire, Long-term behavior of oil-based varnishes and paints: photo- and thermooxidation of cured linseed oil, J. Am. Oil Chemists' Soc. 77 (3) (2000) 257–263.